

QUT Digital Repository:
<http://eprints.qut.edu.au/>



This is the accepted version of this article. Published as:

Frost, Ray L. and Bahfenne, Silmarilly and Keefe, Eloise C. (2009) *Raman spectroscopic study of the antimonate mineral brandholzite Mg[Sb(OH)6].6H2O*. *Journal of Raman Spectroscopy*, 40(12). pp. 1907-1910.

© Copyright 2009 John Wiley & Sons, Ltd.

The definitive version is available at www3.interscience.wiley.com

1 **Raman spectroscopic study of the antimonate mineral brandholzite**
2 **Mg[Sb(OH)₆]·6H₂O**

3
4
5 **Ray L. Frost,¹ • Jiří Čejka,^{1,2} Jiří Sejkora,²**
6 **Daniel Ozdín,³ Silmarilly Bahfenne and Eloise C. Keeffe¹**

7
8
9
10 ¹ Inorganic Materials Research Program, School of Physical and Chemical
11 Sciences, Queensland University of Technology, GPO Box 2434, Brisbane
12 Queensland 4001, Australia.

13
14 ² National Museum, Václavské náměstí 68, CZ-115 79 Praha 1, Czech Republic.

15
16 ³ Department of Mineralogy and Petrology, Faculty of Science, Comenius University,
17 Mlynská Dolina, SK-84 215, Bratislava, Slovak Republic

18
19
20
21
22 **Raman spectra of brandholzite Mg[Sb(OH)₆]·6H₂O were studied,**
23 **complemented with infrared spectra, and related to the structure of the**
24 **mineral. An intense Raman sharp band at 618 cm⁻¹ is attributed to the SbO**
25 **symmetric stretching mode. The low intensity band at 730 cm⁻¹ is ascribed to**
26 **the SbO antisymmetric stretching vibration. Low intensity Raman bands were**
27 **found at 503, 526 and 578 cm⁻¹. Corresponding infrared bands were observed**
28 **at 527, 600, 637, 693, 741 and 788 cm⁻¹. Four Raman bands observed at 1043,**
29 **1092, 1160 and 1189 cm⁻¹ and eight infrared bands at 963, 1027, 1055, 1075,**
30 **1108, 1128, 1156 and 1196 cm⁻¹ are assigned to δ SbOH deformation modes. A**
31 **complex pattern resulting from the overlapping band of the water and**
32 **hydroxyl units is observed. Raman bands are observed at 3240, 3383, 3466,**
33 **3483 and 3552 cm⁻¹, infrared bands at 3248, 3434 and 3565 cm⁻¹. The first two**
34 **Raman bands and the first infrared band are assigned to water stretching**
35 **vibrations. The two higher wavenumber Raman bands observed at 3466 and**
36 **3552 cm⁻¹ and two infrared bands at 3434 and 3565 cm⁻¹ are assigned to the**
37 **stretching vibrations of the hydroxyl units. Observed Raman and infrared**
38 **bands are connected with O-H...O hydrogen bonds and their lengths 2.72,**
39 **2.79, 2.86, 2.88 and 3.0 Å (Raman) and 2.73, 2.83 and 3.07 Å (infrared).**

40
41 **Keywords:** brandholzite, antimonate, antimonite, molecular water, Raman, infrared,
42 spectroscopy

43
44 **Introduction**

45
46 The mineral brandholzite, trigonal MgSb₂(OH)₁₂·6H₂O, was originally
47 described as plate-like crystals up to 1 mm in size in association with stibnite from
48 mining district Brandholz-Goldkronach (Bavaria, Germany)¹. Later, it was also

• Author to whom correspondence should be addressed (r.frost@qut.edu.au)

49 found as tiny colorless aggregates at the Krížnica mine, the Pernek deposit, the Malé
50 Karpaty Mountains, western Slovakia, Slovak Republic ^{2,3} in association with stibnite,
51 sulphur, aragonite, gypsum and antimony-ochres. The structure of the mineral has
52 been published ^{1,4}. Its crystal structure is isotypic with bottinoite ^{5,6}. The mineral is
53 isotypic with synthetic $\text{Co}(\text{H}_2\text{O})_6[\text{Sb}(\text{OH})_6]_2$ ⁴ and bottinoite, $\text{Ni}(\text{H}_2\text{O})_6[\text{Sb}(\text{OH})_6]_2$ ⁵⁻⁷.

54
55 Farmer reported the infrared spectra of some synthetic antimonite minerals
56 (see page 413 and 414 with Tables 17. XVIII and XIX) ⁸. For the synthetic
57 compound $\text{NaSb}(\text{OH})_6$ which is a compound with an octahedral structure, infrared
58 bands were observed at 600 and 628 cm^{-1} (very intense), 735, 775 cm^{-1} (medium
59 intensity), and 528 and 586 cm^{-1} . Siebert researched the infrared spectra of selected
60 synthetic antimonates ^{9,10}. Siebert assigned bands in the 528 to 775 cm^{-1} region to the
61 stretching vibrations of SbO units; in the 1030 to 1120 cm^{-1} to the deformation modes
62 of SbOH units and in the 3220 to 3400 cm^{-1} to the stretching bands of SbOH and
63 water units.

64
65 It is interesting to note that only very few papers have been published on the
66 spectroscopy of antimonate minerals. What research has been published is related to
67 the analysis of pigments ¹¹⁻¹³. Some spectroscopic studies of calcium and lead
68 antimonates have been forthcoming ¹⁴⁻¹⁶. Very few studies of related minerals such as
69 mineral antimonates have not been undertaken ¹⁷⁻¹⁹. It was found that the hydroxyl
70 unit was coordinated directly to the metal ion and formed hydrogen bonds to the
71 arsenate anion ²⁰. Raman spectroscopy has proven especially useful for the study of
72 related minerals ²¹⁻²⁹. As part of a comprehensive study of the molecular structure of
73 secondary minerals containing oxy-anions ³⁰⁻⁴⁰, formed in the oxide zone, using IR
74 and Raman spectroscopy, we report the Raman properties of the antimonate mineral
75 brandholzite. The spectra are related to the mineral structure.

76 77 78 **Experimental**

79 80 **Mineral**

81
82 The studied sample of the mineral brandholzite was found at Krížnica mine,
83 the Pernek deposit, the Malé Karpaty Mountains, western Slovakia, Slovak Republic
84 [39], and is deposited in the mineralogical collections of the National Museum
85 Prague. The sample was analysed for phase purity by X-ray powder diffraction. No
86 minor significant impurities were found. Its refined unit-cell parameters for trigonal
87 space group $P3$, a 16.1076(9), c 9.8628(9) Å, V 2216.1(2) Å³, are comparable with
88 the data published for this mineral phase ¹. The mineral was analysed by electron
89 microprobe (Cameca SX100, WD mode) for chemical composition. The results (mean
90 of 2 point analyses, recalculation to 100 wt. %) are MgO 6.11, CaO 0.52, FeO 0.16,
91 Sb_2O_5 55.91, H_2O 37.30 wt. %, sum 100.00 wt. %. The water content was calculated
92 on the basis of theoretical content (OH) = 12 and H_2O = 6 *pfu*. The resulting empirical
93 formula is $(\text{Mg}_{0.88}\text{Ca}_{0.06}\text{Fe}_{0.01})_{\Sigma 0.95}(\text{H}_2\text{O})_{6.00}[\text{Sb}(\text{OH})_6]_{\Sigma 2.01}$.

94 95 **Raman spectroscopy**

96
97 The crystals of brandholzite were placed and oriented on the stage of an
98 Olympus BHSM microscope, equipped with 10x and 50x objectives and part of a

99 Renishaw 1000 Raman microscope system, which also includes a monochromator, a
100 filter system and a Charge Coupled Device (CCD). Further details have been
101 published ²¹⁻²⁹.

102 IR spectroscopy

103 The FTIR spectrum of brandholzite was obtained with the FTIR Nicolet 740
104 spectrometer using the conventional KBr-disk technique. Infrared spectrum in the
105 range 4000-400 cm^{-1} was obtained by the co-addition of 32 scans with a resolution of
106 2 cm^{-1} and a mirror velocity of 0.1496 cm/s . Spectral manipulation such as baseline
107 adjustment, smoothing and normalization were performed using the OMNIC software
108 package (Thermo Electron Corporation). Band component analysis was undertaken
109 using the same software package which enabled the type of fitting function to be
110 selected and allows specific parameters to be fixed or varied accordingly. Band fitting
111 was done using a Lorentz-Gauss cross-product function with the minimum number of
112 component bands used for the fitting process which was undertaken until
113 reproducible results were obtained with minimum value of standard errors (usually
114 lower than 2, the range for brandholzite spectra is 1.30-0.20).

115 Results and discussion

116

117 Raman spectroscopy

118

119 The Raman spectrum of brandholzite in the 400 to 800 cm^{-1} region is shown in
120 Fig. 1. The spectrum shows some complexity with a number of overlapping bands
121 observed at 618, 630 and 730 cm^{-1} with additional low intensity bands found at 503,
122 526 and 578 cm^{-1} . Infrared bands were observed at 527, 600, 637, 693, 741 and 788
123 cm^{-1} (Supplementary Figure 1S). According to Siebert ^{9,10} all bands in these positions
124 are assignable to stretching vibrations. The observation of multiple bands in the
125 Raman spectrum provides evidence for the non-equivalence of SbO units in the
126 brandholzite structure. In the infrared spectrum of antimony pentoxide an intense
127 band is observed at 740 cm^{-1} and low intensity bands at ~370, 450 and 680 cm^{-1} ⁴¹.
128 The infrared spectrum of valentinite (Sb_2O_3)₄ showed bands in similar positions ⁴¹.
129 Farmer reported the band positions of synthetic antimonates of formula MSbO_4 where
130 M is Cr, Fe, Ga or Rh with a rutile type structure ⁸. As such these structures should
131 have four Raman active bands ($A_{1g} + B_{1g} + B_{2g} + E_g$) and four infrared active bands
132 ($A_{2u} + 3E_u$). Infrared bands were observed in the 660 to 735 cm^{-1} , 520 to 585 cm^{-1} ,
133 285 to 375 cm^{-1} and 170 to 190 cm^{-1} . Although no assignment was given to these
134 bands but one possible interpretation is that the first band is attributed to the
135 antisymmetric stretching mode, the second to the symmetric stretching mode, the
136 third to bending modes and the fourth to a lattice modes. Hence the bands of
137 brandholzite at around 618 cm^{-1} are attributable the symmetric stretching modes. The
138 observation of several bands in this region suggests that the $\text{Sb}(\text{OH})_6^{2-}$ are not
139 equivalent. In the infrared spectrum of the compound $\text{NaSb}(\text{OH})_6$ which has an
140 octahedral structure, a very intense band is observed at 628 cm^{-1} with bands of lower
141 intensity at 775 and 528 cm^{-1} ⁸.

142

143 The Raman spectrum of brandholzite in the 100 to 400 cm^{-1} region is
144 displayed in Figure 2. Intense Raman bands are observed at 303, 318 and 340 cm^{-1} .
145 One likely assignment of these bands is to OSbO bending modes. Such an assessment
146 fits well with the assignment of bands for MSbO_4 structures as reported by Farmer ⁸.
147 The observation of multiple bands suggests the non-equivalence of SbO units in the

148 brandholzite structure. Other low intensity bands are observed at 115, 147, 191, 232
149 and 252 cm^{-1} . Low wavenumber bands are observed for MSbO_4 ⁸.

150

151 Raman bands in the 900 to 1800 cm^{-1} region are reported in Fig. 3. Raman
152 bands in this spectral region are of a very low intensity. (The scaling factor is x7000
153 in Fig. 3) Two sets of bands are observed (a) in the 1000 to 1200 cm^{-1} region and (b)
154 centred upon 1648 cm^{-1} . Four Raman bands are observed at 1043, 1092, 1160 and
155 1189 cm^{-1} . Eight infrared bands at 963, 1027, 1055, 1075, 1108, 1128, 1156 and 1196
156 cm^{-1} were observed (Supplementary information Figure 2S). These bands are assigned
157 to δ SbOH deformation modes. Siebert reported four infrared bands at 1030, 1075,
158 1105 and 1120 cm^{-1} for the synthetic compound NaSb(OH)_6 . The position and
159 number of these infrared bands for his compound is in good agreement with the
160 position of the Raman bands of brandholzite. The Raman band at 1648 cm^{-1} is
161 ascribed to the water HOH bending mode. The position of the band for liquid water is
162 $\sim 1630 \text{ cm}^{-1}$. The position of the band at 1648 cm^{-1} and infrared bands at 1632 and
163 1653 cm^{-1} (Supplementary information Figure 3S) provides evidence for the water
164 being strongly hydrogen-bonded in the brandholzite structure. Weak infrared bands at
165 1541, 1558 and 1739 cm^{-1} may be probably connected with overtones and/or
166 combination bands.

167

168

169 The Raman spectrum of brandholzite in the 2600 to 3800 cm^{-1} region is
170 shown in Figure 4. A complex pattern resulting from the overlapping bands of the
171 water and OH units is observed. Raman bands are observed at 3240, 3383, 3466,
172 3483 and 3552 cm^{-1} , infrared bands at 3248, 3434 and 3565 cm^{-1} . The Raman bands
173 at 3240 and 3383 cm^{-1} and the infrared band at 3248 cm^{-1} are assigned to water
174 stretching vibrations. The higher wavenumber bands observed at 3466 and 3552 cm^{-1}
175 (Raman) and 3434 and 3565 cm^{-1} (infrared) (Supplementary information Figure 4S)
176 are assigned to the stretching vibrations of the OH units. There may be inferred a
177 hydrogen-bonding network in the crystal structure of brandholzite with corresponding
178 O-H...O hydrogen bond lengths⁴² 2.72, 2.79, 2.86, 2.88 and 3.0 Å [Raman], and
179 2.73, 2.83 and 3.07 Å (infrared).

180

181

182 CONCLUSIONS

183 Raman spectra of brandholzite $\text{Mg}[\text{Sb(OH)}_6] \cdot 6\text{H}_2\text{O}$ have been studied and
184 related to the structure of the mineral. Raman bands were assigned SbO stretching
185 modes, δ SbOH deformation modes, OH stretching modes and water stretching and
186 bending modes. O-H...O hydrogen bond lengths in the crystal structure of
187 brandholzite were inferred from the Raman and infrared spectra.

188

189

190

191

192

193 Acknowledgments

194 This work was supported by Ministry of Culture of the Czech Republic
195 (project MK00002327201) to Jiří Sejkora. The authors thank to Miroslava Novotná
196 (VŠCHT, Prague) for her kind support of recording the IR spectrum of brandholzite.

197 The financial and infra-structure support of the Queensland University of Technology,
198 Inorganic Materials Research Program is gratefully acknowledged. The Australian
199 Research Council (ARC) is thanked for funding the instrumentation.
200
201

202 **References**

203

- 204 (1) Friedrich A, Wildner M, Tillmanns E, Merz PL *American Mineralogist* **2000**,
205 85, 593-599.
- 206 (2) Sejkora J, Ozdín D, Vitáloš J, R. Ďud'a *Journal of Geosciences*.
- 207 (3) Sejkora S, Ozdín D, Vitáloš J, Tuček P, Ďud'a R *Lapis* **2004**, 29, 27-36.
- 208 (4) Friedrich A, Mazzi F, Wildner M, Tillmanns E *American Mineralogist* **2003**,
209 88, 462-463.
- 210 (5) Bonazzi P, Mazzi F *American Mineralogist* **1996**, 81, 1494-1500.
- 211 (6) Bonazzi P, Menchetti S, Caneschi A, Magnanelli S *American Mineralogist*
212 **1992**, 77, 1301-4.
- 213 (7) Clark AM, Rust SA *Mineralogical Magazine* **1993**, 57, 543-4.
- 214 (8) Farmer VC *Mineralogical Society Monograph 4: The Infrared Spectra of*
215 *Minerals*, 1974.
- 216 (9) Siebert H *Z. anorg. u. allgem. Chem.* **1959**, 301, 161-70.
- 217 (10) Siebert H *Anwendungen der Schwingungsspektroskopie in der Anorganischen*
218 *Chemie (Anorganische und Allgemeine Chemie in Einzeldarstellungen, Bd. 7)*
219 *(Application of Vibrational Spectroscopy in Inorganic Chemistry (Monographs in*
220 *Inorganic and General Chemistry, Vol. 7))*, 1966.
- 221 (11) Correia AM, Oliveira MJV, Clark RJH, Ribeiro MI, Duarte ML *Analytical*
222 *Chemistry (Washington, DC, United States)* **2008**, 80, 1482-1492.
- 223 (12) Correia AM, Clark RJH, Ribeiro MIM, Duarte MLTS *Journal of Raman*
224 *Spectroscopy* **2007**, 38, 1390-1405.
- 225 (13) Clark RJH, Cridland L, Kariuki BM, Harris KDM, Withnall R *Journal of the*
226 *Chemical Society, Dalton Transactions: Inorganic Chemistry* **1995**, 2577-82.
- 227 (14) Husson E, Repelin Y, Vandendorre MT *Spectrochimica Acta, Part A:*
228 *Molecular and Biomolecular Spectroscopy* **1984**, 40A, 1017-20.
- 229 (15) Haeuseler H *Spectrochimica Acta, Part A: Molecular and Biomolecular*
230 *Spectroscopy* **1981**, 37A, 487-95.
- 231 (16) Vandendorre MT, Husson E, Brusset H, Cerez A *Spectrochimica Acta, Part*
232 *A: Molecular and Biomolecular Spectroscopy* **1980**, 36A, 1045-52.
- 233 (17) Paques-Ledent MT, Tarte P *Spectrochim. Acta, Part A* **1974**, 30A, 673-89.
- 234 (18) Gevork'yan SV, Povarennykh AS *Konst. Svoistva Miner.* **1975**, 9, 73-81.
- 235 (19) Braithwaite RSW *Mineral. Mag.* **1983**, 47, 51-7.
- 236 (20) Sumin De Portilla VI *Can. Mineral.* **1974**, 12, 262-8.
- 237 (21) Frost RL, Cejka J, Ayoko G *Journal of Raman Spectroscopy* **2008**, 39, 495-
238 502.
- 239 (22) Frost RL, Cejka J, Ayoko GA, Dickfos MJ *Journal of Raman Spectroscopy*
240 **2008**, 39, 374-379.
- 241 (23) Frost RL, Cejka J, Dickfos MJ *Journal of Raman Spectroscopy* **2008**, 39, 779-
242 785.
- 243 (24) Frost RL, Dickfos MJ, Cejka J *Journal of Raman Spectroscopy* **2008**, 39, 582-
244 586.
- 245 (25) Frost RL, Hales MC, Wain DL *Journal of Raman Spectroscopy* **2008**, 39, 108-
246 114.
- 247 (26) Frost RL, Keeffe EC *Journal of Raman Spectroscopy* **2008**, in press.
- 248 (27) Frost RL, Locke A, Martens WN *Journal of Raman Spectroscopy* **2008**, 39,
249 901-908.
- 250 (28) Frost RL, Reddy BJ, Dickfos MJ *Journal of Raman Spectroscopy* **2008**, 39,
251 909-913.

- 252 (29) Palmer SJ, Frost RL, Ayoko G, Nguyen T *Journal of Raman Spectroscopy*
253 **2008**, 39, 395-401.
- 254 (30) Frost RL, Bouzaid JM *Journal of Raman Spectroscopy* **2007**, 38, 873-879.
- 255 (31) Frost RL, Bouzaid JM, Martens WN, Reddy BJ *Journal of Raman*
256 *Spectroscopy* **2007**, 38, 135-141.
- 257 (32) Frost RL, Cejka J *Journal of Raman Spectroscopy* **2007**, 38, 1488-1493.
- 258 (33) Frost RL, Cejka J, Ayoko GA, Weier ML *Journal of Raman Spectroscopy*
259 **2007**, 38, 1311-1319.
- 260 (34) Frost RL, Cejka J, Weier ML *Journal of Raman Spectroscopy* **2007**, 38, 460-
261 466.
- 262 (35) Frost RL, Cejka J, Weier ML, Martens WN, Ayoko GA *Journal of Raman*
263 *Spectroscopy* **2007**, 38, 398-409.
- 264 (36) Frost RL, Dickfos MJ *Journal of Raman Spectroscopy* **2007**, 38, 1516-1522.
- 265 (37) Frost RL, Palmer SJ, Bouzaid JM, Reddy BJ *Journal of Raman Spectroscopy*
266 **2007**, 38, 68-77.
- 267 (38) Frost RL, Pinto C *Journal of Raman Spectroscopy* **2007**, 38, 841-845.
- 268 (39) Frost RL, Weier ML, Williams PA, Leverett P, Kloprogge JT *Journal of*
269 *Raman Spectroscopy* **2007**, 38, 574-583.
- 270 (40) Locke AJ, Martens WN, Frost RL *Journal of Raman Spectroscopy* **2007**, 38,
271 1429-1435.
- 272 (41) Gadsden JA *Infrared spectra of minerals and related inorganic compounds*;
273 Butterworth: London, UK, 1975.
- 274 (42) Libowitzky E *Monatshefte fuer Chemie* **1999**, 130, 1047-1059.
275
276
277

278 ***List of Figures***

279

280 Fig. 1 Raman spectrum of brandholzite in the 600 to 1200 cm^{-1} region

281

282 Fig. 2 Raman spectrum of brandholzite in the 100 to 600 cm^{-1} region

283

284 Fig. 3 Raman spectrum of brandholzite in the 1200 to 1800 cm^{-1} region

285

286 Fig. 4 Raman spectrum of brandholzite in the 3000 to 3700 cm^{-1} region

287

288

289 Fig. S1 Infrared spectrum of brandholzite in the 490 to 900 cm^{-1} region

290

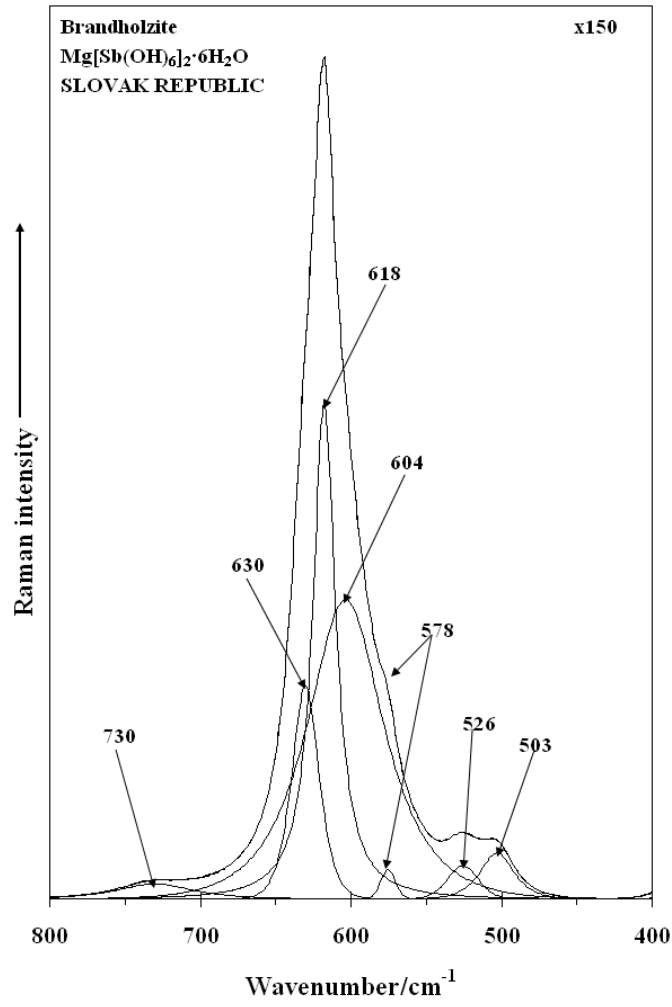
291 Fig. S1 Infrared spectrum of brandholzite in the 910 to 1240 cm^{-1} region

292

293 Fig. S1 Infrared spectrum of brandholzite in the 1490 to 1800 cm^{-1} region

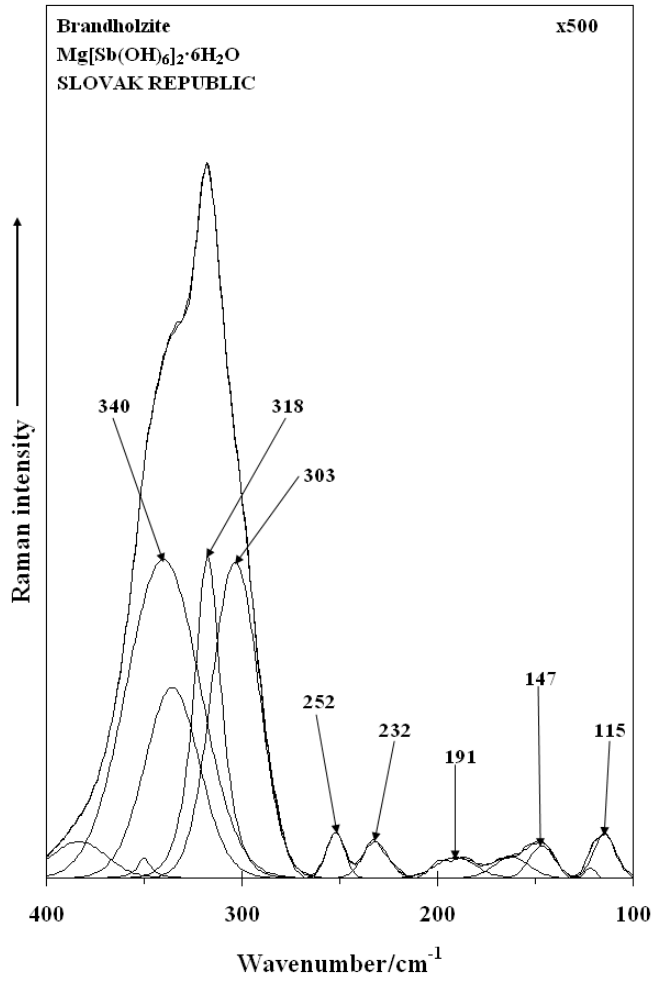
294

295 Fig. S1 Infrared spectrum of brandholzite in the 2600 to 3850 cm^{-1} region



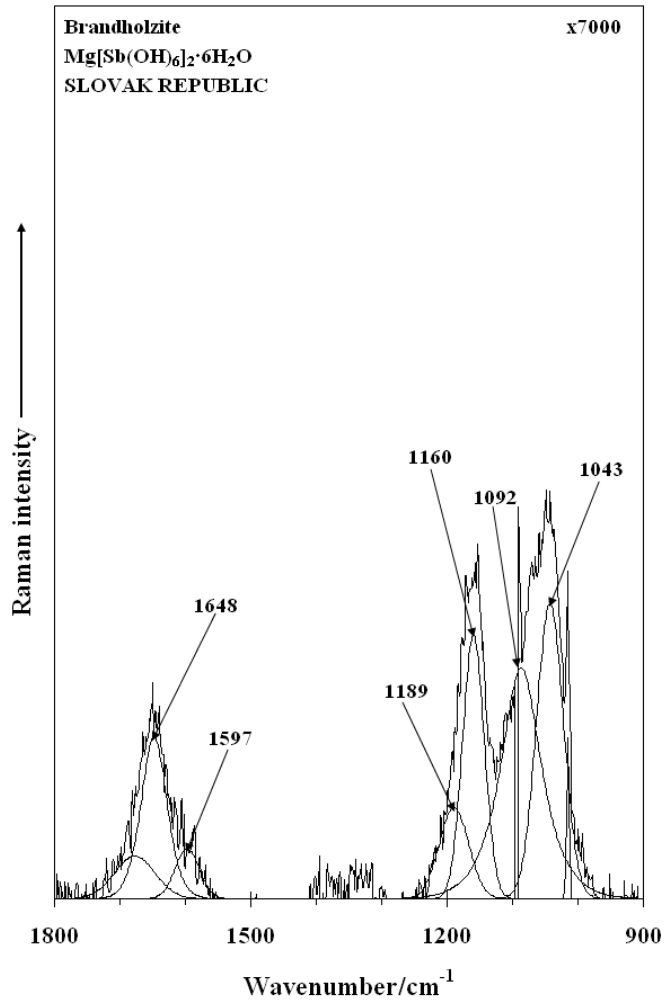
296
297
298
299
300
301

Figure 1



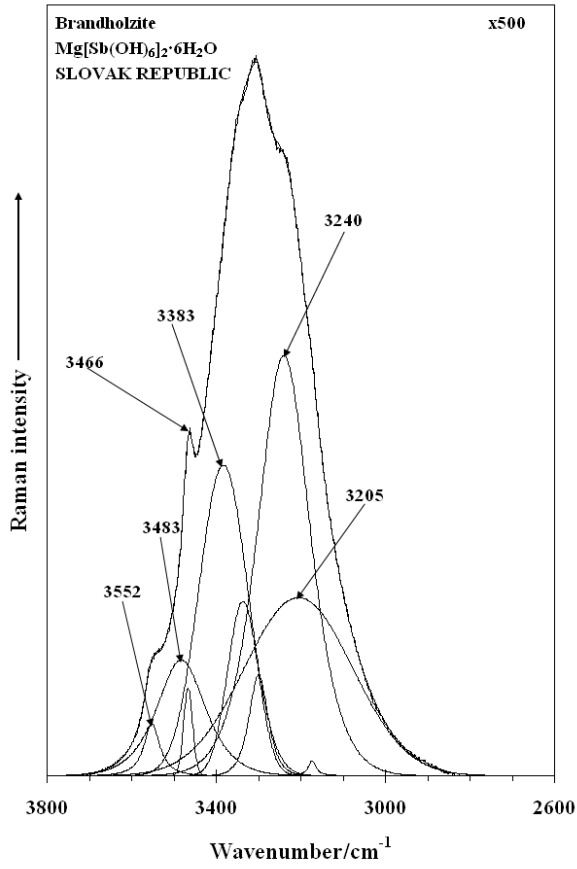
302
 303
 304
 305
 306

Figure 2



307
308
309
310
311

Figure 3



312
313
314

Figure 4